

Integrated cavity output spectroscopy by using a sub-centimeter short optical cavity combined with a free-running Fabry–Perot diode laser

Xiutao Lou^{1,2} · Yongkang Dong² · Dongcheng Wu¹ · Jiatian Wei¹ · Zhiwei Lu²

Received: 24 December 2014 / Accepted: 29 August 2015 / Published online: 9 September 2015
© Springer-Verlag Berlin Heidelberg 2015

Abstract In integrated cavity output spectroscopy (ICOS), a long optical cavity is often required for suppressing mode structure, which, however, blocks its application for fabricating compact gas sensors requiring gas cells with the volume at milliliter level or less. In this paper, we demonstrate that low-cost free-running Fabry–Perot diode lasers have intrinsic capability for promoting suppression of cavity resonance due to the broad linewidth. The ICOS is performed, for the first time to our best knowledge, by using a short cavity of less than 1 cm with a cavity volume of only 4.7 cm³. By introduction of the scheme of correlation spectroscopy, the problem of laser mode competitions is resolved. A minimum detectable absorption of $8.7 \times 10^{-5} \text{ Hz}^{-1/2}$ (noise-equivalent absorption sensitivity of $3.3 \times 10^{-7} \text{ cm}^{-1} \text{ Hz}^{-1/2}$) is achieved. The performance is suitable for applications in which both high sensitivity and small gas cell volume are required.

1 Introduction

In laser absorption spectroscopy (LAS), sensitivity is a crucial factor for unambiguous detection and quantification of trace gas species [1, 2]. Higher levels of sensitivity can be achieved by extending the absorption pathlength through folding laser beams in particularly designed gas cells. Typical embodiments include multipass cells [3, 4], high-finesse optical cavities [5, 6], integrating spheres [7, 8] and porous scattering media [9, 10]. Because of the recent enormous advances in optoelectronics, the optical gas cell often becomes the bottleneck for configuring a compact gas sensor for applications in which the amount of sample gas is limited [11, 12] or the volume of the gas sensor itself is restricted [13]. Recently, a compact multipass cell based on a near-concentric cavity with a pathlength of 4.1 m and a volume of 40 cm³ has been proposed [4]. However, it requires high beam quality and time-consuming alignment. Among the various pathlength enhancement methods, high-finesse optical cavity-based techniques [5, 14, 15] can achieve the largest enhancement factor and thus would in principle be the best choice for fabricating compact gas sensors.

In field applications, the integrated cavity output spectroscopy (ICOS) is often preferred because it removes the need of active frequency locking, thus possessing advantages of simple alignment and mechanical robustness. The ICOS is typically based on an off-axis cavity alignment by using a relatively long optical cavity and/or combined with a pair of large diameter mirrors to create extremely dense mode structure [16]. In this case, the mode spacing is well below the laser linewidth so that the cavity becomes mostly non-resonant. However, this requirement is rarely fulfilled to fabricate compact gas sensors using short cavities. For instance, for effectively analyzing human breath the cell

✉ Xiutao Lou
louxiutao@hit.edu.cn
Yongkang Dong
aldendong@gmail.com
Zhiwei Lu
zw_lu@sohu.com

¹ Department of Physics, Harbin Institute of Technology, Harbin 150001, China

² National Key Laboratory of Science and Technology on Tunable Laser, Harbin Institute of Technology, Harbin 150001, China

volume of an analyzer should be less than 100 cm^3 . Bakhirkin et al. [17] reported an OA-ICOS-based breath analyzer with a cavity length of 5.3 cm, while the diameter of the mirror was relatively large (5.08 cm) to reduce the cavity mode spacing. Common methods for promoting the suppression of the cavity resonance rely on randomizing the cavity mode structure through dithering the cavity length or modulating the laser injection current [14]. Recently, Ciaffoni and Manfred et al. reported a new resonance-suppression strategy based on the reduction of laser coherence length [18, 19]. In their work, by perturbing the laser frequency with radio frequency (RF) white noise the linewidth of a vertical-cavity surface-emitting laser (VCSEL) was increased from 100 to over 500 MHz and the linewidth of a mid-IR quantum cascade laser was increased from 6 to 27 MHz.

In this paper, we demonstrate that low-cost free-running Fabry–Perot multimode diode lasers have intrinsic capability for suppressing cavity resonance because of their relatively broad linewidth ($>100 \text{ MHz}$) of the individual mode. The ICOS is performed here for the first time by using a short cavity of less than 1 cm.

Recently, the strategy multimode absorption spectroscopy (MUMAS) that also uses multimode diode lasers as the light source has been reported [20]. This technique is based on simultaneously tuning all the longitudinal modes of the diode laser over a mode interval and detecting the reduction in total transmitted intensity resulting from any individual mode that comes into resonance with an absorbing molecular transition. Despite the requirement of a well-behaved laser source, MUMAS offers the advantage of high spectral resolution and wide spectral coverage using only a single laser and a single detector. MUMAS has recently been successfully combined with the technique of ICOS as well as the strategy of wavelength modulation spectroscopy (WMS) [21]. Although the signal-to-noise ratio (SNR) enhancement achieved was below expectation due to the low power of the laser source, it explicitly indicated the great potential for sensitivity improvement by combining ICOS and WMS.

In general, the spectral linewidth of a FP diode laser is larger by two order of magnitude than those commonly used in ICOS such as distributed feedback (DFB) laser [22] and external cavity diode laser (ECDL) [16], while the price of the former is lower by more than two order of magnitude. Furthermore, compared with VCSELs, FP diode lasers can offer a two-order-of-magnitude larger output power which is particularly beneficial when high-finesse cavities are employed. Usually, FP diode lasers are not preferable for LAS due to their multimode emission and accidental mode hops; therefore, the scheme of correlation spectroscopy (COSPEC) [23, 24] is employed in this work

to guarantee the measurement specificity and accuracy. A FP diode laser with only two major modes is employed so that the dilution of absorption signal magnitude due to laser modes without absorption is downscaled, guaranteeing the measurement sensitivity. In order to promote the suppression of the residual mode structure, off-axis configuration is implemented with the cavity length dithered. Strategy of WMS, which has been proven to be capable of further enhancing the sensitivity by an order of magnitude [25–27], is also exploited.

2 Approaches

2.1 Off-axis ICOS

The technical details of off-axis ICOS have been presented previously [16, 25]. We highlight here only the relevant aspects for signal enhancement and noise suppression. Common to other cavity-enhanced techniques, high sensitivity of ICOS is achieved by using a high-finesse optical cavity in which light travels forth and back yielding an effective optical pathlength

$$L_{\text{eff}} = \frac{L}{1 - R + \alpha L}, \quad (1)$$

where L is the cavity length, R is the mirror reflectivity and α is the per-pass intracavity absorption coefficient. Compared with the cavity length, the effectivity absorption pathlength is gained by a factor of $1/(1 - R + \alpha L)$. For weak absorption ($\alpha L \ll 1 - R$), the gain factor becomes $1/(1 - R)$.

Ideally, the coupling between the laser and the cavity can be considered non-resonant so that there is no structure in the cavity transmission. However, in practice, this goal is not achieved. For most OA-ICOS systems, mode injection noise due to fluctuations in laser coupling is the dominant limitation on spectroscopic sensitivity. According to the theory presented in [25], the mode injection noise can be expressed as:

$$\delta I = \frac{I_0 T^2 c}{4mL\gamma_{\text{las}}\sqrt{\pi(1 - R)}}, \quad (2)$$

where I_0 is the incident light intensity, T is the mirror transmittance, c is the light speed, m is the number of light passes before the reentrant condition is attained, and γ_{las} is the laser linewidth. According to Eq. (2), for an OA-ICOS system with a certain cavity finesse there would be three approaches to suppress the mode injection noise: (1) increase the number of light round trips m by using cavity mirrors with a big diameter; (2) increase the cavity length

L ; (3) employ a laser with a broad linewidth γ_{las} . Although the first and the second methods are straightforward to perform, they are not suitable for applications where a compact gas sensor is required. On the other hand, the third method would be a good choice when the volume of the gas cell is restricted.

2.2 COSPEC

The laser-based COSPEC technique is based on time correlation [28], and thus detailed wavelength is no longer needed. By comparing the recorded absorption spectrum of the sample gas with that of the particular reference gas of interest, we can identify the presence of the target gas in the sample and calculate its concentration. The measurement selectivity lies in the unique spectral signature of the target gas: The sample and the reference signals originating from the same species of gas would be well correlated both in line shape and in magnitude ratio. The correlation can be well maintained even when different laser modes simultaneously come into resonance with multiple gas absorption lines, since total absorption is just a mode-power-weighted linear superposition of the individual absorptions by each laser mode [23]. Signals originating from disturbances including interfering gases and mode hops are independent of the presence of the target gas and thus can be readily discriminated.

When performing COSPEC, an issue that needs to be concerned is the lineshape distortion experienced in cavity-enhanced systems due to the exponential pathlength distributions [29]. To meet the requirement for COSPEC that the signal line shapes of the analyte in both sample and reference gases are the same, all experiments in this work were performed at low absorption regime where lineshape distortion can be neglected. In condition of high absorptions, a correction model can be established to correct the measurement results [23]. Another issue relating to the lineshape distortion is the broadening of the acquired absorption spectrum when a laser with broad linewidth is used. The broadening of absorption signal would lead to a reduction in spectral resolution. However, since the lineshape distortion in the sample and the reference channel is identical, it will not much affect the measurement results.

3 Experimental setup

Our experimental setup is schematically shown in Fig. 1. The oxygen in the laboratory open air was measured as a demonstration. The FP diode laser (Qphotonics, LD-760-10S) employed has a maximum output power of 10 mW and an emission wavelength near 760 nm where there

are abundant oxygen A-band absorption lines, according to high-resolution transmission molecular absorption database (HITRAN). The laser wavelength was repeatedly scanned by a 16-Hz current ramp through a diode laser driver (Thorlabs, LDC205). The operating temperature of the laser was controlled by a temperature controller (Thorlabs, TED200C). To perform COSPEC, after collimation the laser output was split into two beams with a splitting ratio of $\sim 20:1$ passing through the sample path and the reference path, respectively. In the reference path, following passing through 195.9 cm in the open air the light was detected by a biased Si photodiode (Thorlabs, DET 210). In the sample arm, the laser beam was directed into an optical cavity consisting of two 2.5-cm-diameter concave spherical mirrors of reflectivity $\sim 99.7\%$ and radius of curvature 1 m. The choice of a modest mirror reflectivity was driven by the large absorption coefficient ($\sim 2 \times 10^{-4}/\text{cm}$) of ambient oxygen around 760 nm. A two-stage Faraday isolator with 55 dB isolation and 80% transmission (Thorlabs, IOT-5-780-VLP) was used to minimize the optical feedback from the input cavity mirror into the laser. In fact, the isolator could be placed before the beam splitter to further reduce the optical feedback from the reference path. However, in consideration of the low laser power (a few hundreds of μW) in the reference path and $>20\%$ light attenuation caused by the isolator, the isolator was here placed in the sample path to save the reference laser power. The front cavity mirror mount (Thorlabs, KC1-PZ) with piezoelectric adjusters can provide fast modulation of the cavity length. The light emerging from the output cavity mirror was focused onto a Si transimpedance amplified photodetector (Thorlabs, PDA100A). Although the beam quality of the diode laser employed was poor, as also shown in Fig. 1, no shaping optics was used since the noise coming from mode injection rather than beam interferences would be dominant. The signals in the two arms were simultaneously recorded by a data acquisition card (Adlinktech, DAQ-2010) mounted on a personal computer.

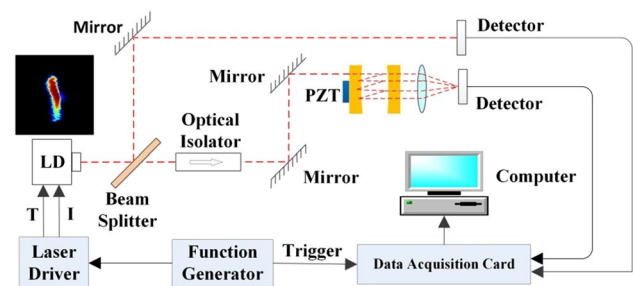


Fig. 1 Schematic diagram of the experimental configuration for oxygen detection in the open air by using short-cavity-based ICOS

4 Measurement results and analysis

4.1 Cavity transmitted spectra

For OA-ICOS method, the actual sensitivity enhancement is basically achieved by smoothing out the cavity mode structure. This can be virtually accomplished in the case of mode spacing well below the laser linewidth. According to Eq. (2), mode injection noise is inversely proportional to laser linewidth. The typical linewidth of commonly used DLs with optical feedbacks such as DFB and ECDL is in the order of 1 MHz or less. The free-running-type MDL used here has typical longitudinal mode linewidth of ~ 100 MHz, and therefore it would in principle cause less mode injection fluctuations.

In order to clearly show the success and advantage of combining FP diode lasers with diverse strategies for suppressing mode injection noise, the final off-axis configuration was transmitted step-by-step from a starting on-axis direct absorption scheme. In the starting step, the laser beam was launched axially into the cavity. An iris was placed in front of the input cavity mirror to downscale

the laser beam diameter from 4 mm to less than 2 mm. A pinhole of 1 mm diameter was axially placed between the two cavity mirrors so that only TEM_{00} modes were excited. Since the wavelength tuning range of the diode laser employed is around 25 GHz, in order to show enough TEM_{00} modes the cavity length was set to be 1.90 cm corresponding to a free spectral range (FSR) of 7.9 GHz. Figure 2a shows the cavity transmission of three groups of modes within a scan period. A schematic setup is also shown in the inset. According to the 7.9 GHz FSR of the cavity, the effective width of the wavelength scan within a scan period is estimated to be about 26.5 GHz. In each mode group, the multimode structure corresponds to the multimode emission of the diode laser employed. The laser emission consists of two main modes contribute to $>90\%$ of the laser output power. The interval between adjacent modes is about 0.5 GHz, which indicates that the mode spacing of the laser is $(m \times 7.9 \pm 0.5)$ GHz where m is a positive integer. By using a spectrometer with 0.01-nm resolution (the measured spectrum is not shown), the mode interval of the laser measures 0.12 nm (62.3 GHz) and is accordingly estimated to be 62.7 $(8 \times 7.9 - 0.5)$ GHz. According to the FSR (7.9 GHz) and finesse (1040) of the

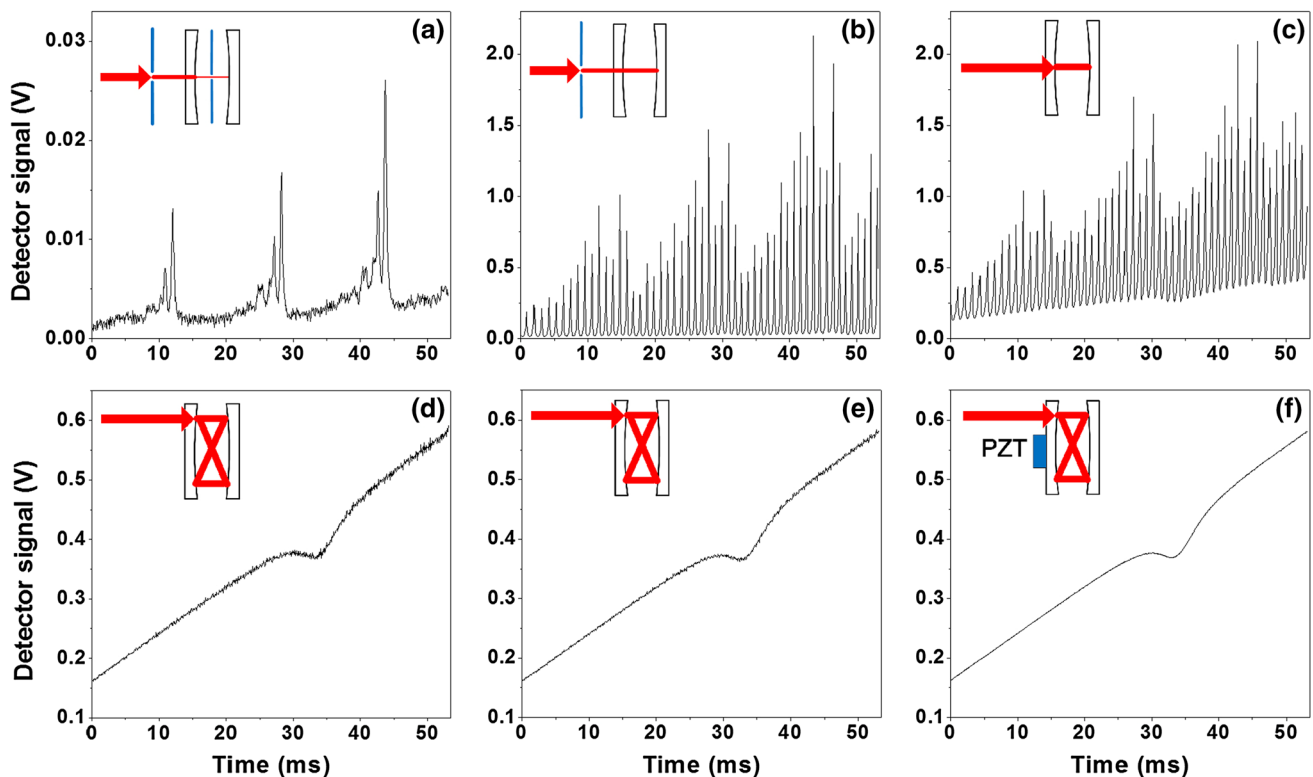


Fig. 2 Transmitted spectra of a 1.90-cm optical cavity with different direct absorption configurations: **a** Only TEM_{00} modes were excited by placing an iris and a pinhole outside and inside the cavity, respectively; **b** high-order cavity modes were excited by removing the pinhole; **c** more transversal cavity modes were excited by removing the

iris to recover the laser beam diameter; **d** extremely dense modes were excited by off-axis configuration; **e** 256-sweep average of the cavity transmission shown in **d**; **f** smoothed spectrum shown in **(e)** by dithering the cavity length using PZTs. The effective width of the wavelength scan within a scan period is about 26.5 GHz

cavity, its optimal spectral resolution is about 8 MHz. The linewidth of each TEM₀₀ mode shown in Fig. 2a is about 190 MHz; accordingly, the linewidth of the laser mode can be estimated to be approximately 180 MHz. Secondly, the pinhole between the cavity mirrors was removed, and high-order cavity modes were excited. Figure 2b shows the 1-sweep cavity transmission in which the gas absorption feature can still not be seen. Thirdly, the iris in front of the cavity was removed, and the laser beam diameter recovered exciting more transversal cavity modes. In this case, the minimum intensity transmission became nonzero, and the absorption feature loomed through the base level of the transmission, as shown in Fig. 2c. In the next and fourth step, off-axis configuration was performed by shifting the laser beam out of the cavity axis by 4 mm. In this approach, the transmitted mode structure became extremely dense so that the absorption feature can be seen clearly, as shown in Fig. 2d. Since the residual mode structure was not stable in time thus can be partially averaged out. Figure 2e shows a 256-sweep (16 s) average of the cavity transmission which is smoother than that shown in Fig. 2d. In the fifth step, the cavity length was dithered by modulating the input cavity mirror through PZTs. Figure 2f shows the cavity transmission with 256-sweep average which is obviously smoother compared with that shown in Fig. 2e.

Up to the fifth step, the configuration of direct-absorption-based ICOS is mainly completed. Then the cavity length was shortened by half to be less than 1 cm and a preparatory analysis of the measurement sensitivity was performed. The sensitivity was characterized by minimum detectable absorption (MDA) defined as the linecenter fractional absorption of a gas concentration equal to the 1σ measurement precision in 1-s integration, which is suggested by Moyer et al. [30] to permit ready comparison of instruments with different designs. Figure 3 shows a pair of absorption signals obtained from the sample and the reference channel, respectively. The absorption signals are evaluated by simultaneously fitting a cubic baseline and a Voigt absorption profile to the cavity transmission. Non-linear Levenberg–Marquardt optimization algorithm is implemented. In order to make fitting robust, parameters of the position and width of the absorption are initialized by using expected values, and their fitted values are 31.1 and 6.2 ms, respectively. The sample signal corresponds to the absorption of ambient air oxygen in the 0.96-cm cavity with a 16-s (256 sweeps) integration time. Judging from the shape of the absorption signal, only one of the two major laser modes interacts with the absorption line of oxygen. By comparison of the absorption amplitudes of the sample and the reference signals, the effective optical pathlength in the optical cavity is determined to be 263.9 cm. According to Eq. (1), the reflectivity of the optical mirror is 99.64 % which is slightly lower

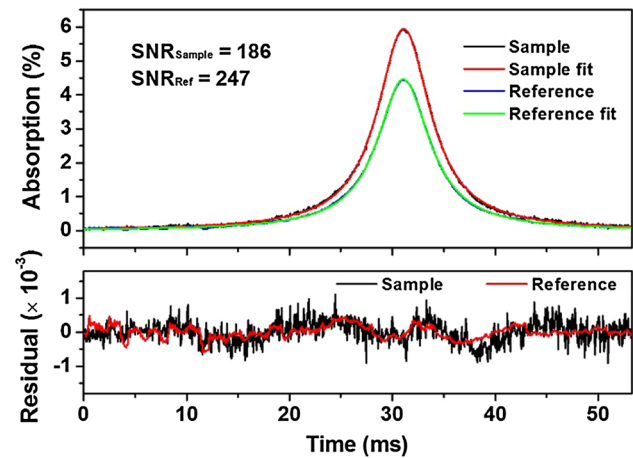


Fig. 3 Pair of direct absorption signals obtained from the sample channel (0.96-cm optical cavity) and reference channel, respectively. The lower panel shows the fit residuals

than the nominal value. Voigt fit profiles and fit residuals are also shown. According to the fit residuals, the MDAs of the sample channel and the reference channel are $1.3 \times 10^{-3} \text{ Hz}^{-1/2}$ and $7.2 \times 10^{-4} \text{ Hz}^{-1/2}$, respectively. The corresponding SNRs are 186 and 247, respectively. The noisy structures in the sample spectrum not present in the reference could be attributed to the mode coupling noise in the cavity.

4.2 Sensitivity improvement by WMS

In order to improve the SNR and thus the sensitivity of the ICOS system, WMS was performed by superimposing a 16-kHz sinusoidal modulation on the 16-Hz current ramp. The modulated signals were demodulated by LabVIEW-based lock-in software at the second harmonic of the modulation frequency ($2f$, 32 kHz) with a time constant of 0.1 ms. The WMS functions here in two aspects: The one is to promote the averaging of mode injection noise by using a fast modulation of the laser wavelength across a number of cavity modes per unit time; the other is to filter optical and electrical noise by narrowing the detection bandwidth around the double frequency of modulation. Figure 4 shows the measured and simulated WMS- $2f$ signals corresponding to the direct absorption signals shown in Fig. 3. Because of the accidental mode hops and variability of the relative mode intensity of FP diode lasers, it is difficult to know which particular absorption lines are being monitored (in fact, there is no need to do so by combination of COSPEC scheme). Therefore, the fitted absorption magnitude and linewidth of the direct absorption signals shown in Fig. 3 were used for the simulation. Other simulation parameters (wavelength scan range 26.5 GHz and modulation index 1.5) were directly based on the experimental settings. The

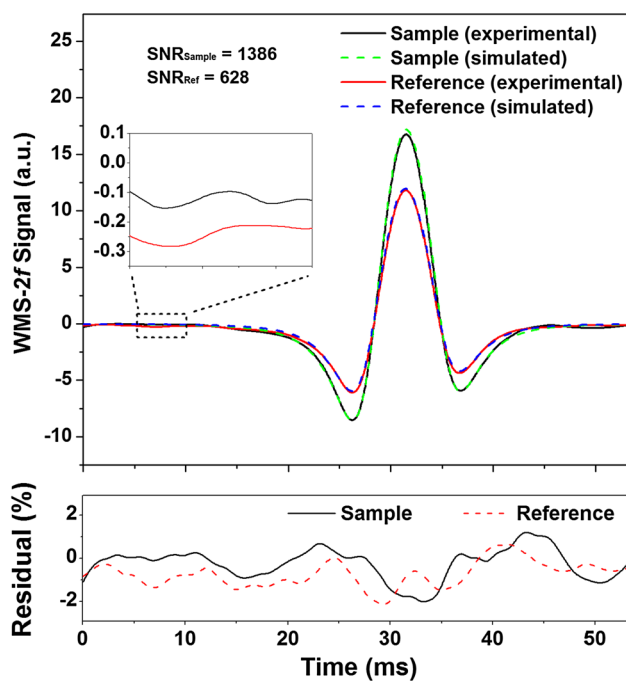


Fig. 4 Measured (solid lines) and simulated (dashed lines) WMS-2f signals corresponding to the direct absorption signals shown in Fig. 3. The lower panel shows the residuals of the simulation

simulation residuals shown in Fig. 4 reveal good agreement (better than 2 %) of the experimental and simulated WMS-2f signatures. The noise level was evaluated by the absorption-free region of the measured WMS-2f signal. An integration time of 4 s was employed here since more averages were not found favorable for improving the sensitivity limited by etalon fringes. The SNRs of the sample and the reference signals are 1386 and 628, respectively, yielding the corresponding MDAs of $8.7 \times 10^{-5} \text{ Hz}^{-1/2}$ and $1.4 \times 10^{-4} \text{ Hz}^{-1/2}$. It indicates that a sensitivity of 150 ppm to oxygen change is achieved for a 4-s integration time. By comparison of the MDA of the sample channel, the sensitivity was improved by a factor of 15 by employment of WMS. The sensitivity achieved in this work is comparable with those obtained by using long cavities, e.g., a MDA of $5.1 \times 10^{-5} \text{ Hz}^{-1/2}$ for WMS-2f signals is reported in [25] by using a 90-cm cavity. Expressing the measurement sensitivity normalized to effective optical pathlength, the noise-equivalent absorption sensitivity ($\text{NEAS} = \text{MDA}/L_{\text{eff}}$) of the sample channel is $3.3 \times 10^{-7} \text{ cm}^{-1} \text{ Hz}^{-1/2}$.

It is worth noting that in the present WM-ICOS the noise level of the sample signal is comparable with that of the reference signal, as shown in the inset of Fig. 4. It means that mode injection noise is effectively suppressed and the poor quality of the laser beam hardly affects the sensitivity performance. Therefore, a higher sensitivity can be

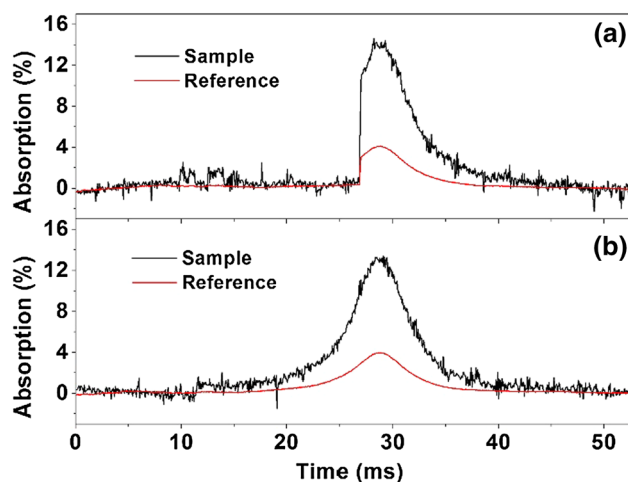


Fig. 5 Captured 1-sweep absorption signal pairs **a** with and **b** without mode-hop perturbation

reasonably expected by using a relatively higher-finesse cavity until the mode injection noise dominates.

4.3 Immunity to laser mode hops

Diode lasers of free-running type have much more chance to encounter mode hops than those with optical feedbacks, which is one of the most important factors hampering their utilization in LAS. Therefore, we finally demonstrate that by introduction of COSPEC scheme occasional mode hops would not affect the measurement accuracy. To make an effortless observation of the mode-hop behavior of the diode laser, its operating temperature was repeatedly varied within a 5 °C range to intensify mode competitions. By employment of COSPEC technique, the concentration of the sample gas is obtained by multiplying the reference concentration by the sample-to-reference magnitude ratio. The absorption amplitude ratio is obtained by fitting the sample signal to the reference signal employing a linear-least-squares fitting method in combination with a multiple-linear-regression fitting approach. As a result, the absorption signal can be well described by a sum of the reference signal multiplied by the fitted amplitude ratio and a quadratic baseline. More details of the fitting procedure can be referred to [23]. Figure 5a, b shows 1-sweep signal pairs of direct absorption with and without perturbation, respectively. The fitted ratios of 3.39 and 3.31 are greatly consistent. The discrepancy mainly comes from the mode injection noise as the signals were captured in a scan period without average. It indicates that by using correlation scheme perturbations from mode hops can be automatically and significantly eliminated, guaranteeing the measurement accuracy and stability [23, 24].

5 Discussion and conclusions

In the described ICOS system, COSPEC technique is employed to deal with the problem of laser mode hops. To guarantee the measurement accuracy, the absorption line shapes of the sample and the reference gas should be identical. Any discrepancy in gas pressures or temperatures would lead to a measurement error. For instance, when performing measurements at around atmospheric pressure, a pressure difference of 0.1 atm can cause relative errors of 3 and 5 % by direct absorption and WMS-2f detection, respectively. For practical applications where atmospheric conditions vary frequently with time, the sample cell can be well controlled to make the temperature and pressure of the sample gas equal to those of sealed reference gas. Alternatively, the reference gas can be sealed in a temperature-controlled gas cell with a moving part (still airtight) to follow the temperature and pressure of the sample gas.

For employment of free-running FP diode lasers, another factor that needs to be considered is the mode-hop-free tuning range of the laser. To our experience, the mode-hop-free tuning range of a FP diode laser is generally more than 5 GHz which is sufficient for acquiring the absorption spectrum of gases analogous to oxygen having sparse narrow lines. In the present work, the laser wavelength can be scanned without mode hops more than 20 GHz. A mode hop might be encountered while the wavelength is scanned across an absorption line. In this case, the measurement sensitivity would be degraded due to the reduction in effective spectral data for analysis; however, the accuracy can still be guaranteed as specified in Sect. 4.3. In the worst case, during a scan period the laser wavelength might not interact with any absorption line, in which condition the operating temperature of the laser needs to be slightly varied to change the scanning range of the laser wavelength.

In conclusion, we have demonstrated the capability of low-cost free-running FP diode lasers with broad linewidth for enhancing the sensitivity of the short-cavity-based ICOS system. The ICOS has been successfully performed for the first time by using a sub-centimeter cavity with a cavity volume of merely 4.7 cm³. The problems relating to multimode emission and mode hops of FP diode laser were resolved by employment of scheme of correlation spectroscopy. The MDA achieved was $8.7 \times 10^{-5} \text{ Hz}^{-1/2}$ (corresponding to a noise-equivalent absorption sensitivity of $3.3 \times 10^{-7} \text{ cm}^{-1} \text{ Hz}^{-1/2}$) which is comparable with that obtained by using long cavities. The approach by employment of FP diode lasers in combination with short cavities provides a valuable alternative to fabricate compact, sensitive and low-cost gas sensors for applications in which the amount of sample gas is limited or the volume of the gas sensor itself is restricted. When there are requirements to further shorten the optical cavity, the measurement

sensitivity could be further improved by perturbing the laser frequency to broaden the laser linewidth [18, 19].

Acknowledgments This work was supported by the Natural Science Foundation of China (NSFC) (Grant 61008027) and the Postdoctoral Scientific Research Developmental Fund of Heilongjiang Province (LBH-Q14069).

References

1. J. Hodgkinson, R.P. Tatam, Optical gas sensing: a review. *Meas. Sci. Technol.* **24**, 012004 (2013)
2. J.S. Li, B.L. Yu, W.X. Zhao, W.D. Chen, A review of signal enhancement and noise reduction techniques for tunable diode laser absorption spectroscopy. *Appl. Spectrosc. Rev.* **49**, 666–691 (2014)
3. J.B. McManus, P.L. Kebabian, W.S. Zahniser, Astigmatic mirror multipass absorption cells for long-path-length spectroscopy. *Appl. Opt.* **34**, 3336–3348 (1995)
4. B. Tuzson, M. Mangold, H. Looser, A. Manninen, L. Emmenegger, Compact multipass optical cell for laser spectroscopy. *Opt. Lett.* **38**, 257–259 (2013)
5. A. O’Keefe, D.A.G. Deacon, Cavity ring-down optical spectrometer for absorption-measurements using pulsed laser sources. *Rev. Sci. Instrum.* **59**, 2544–2551 (1988)
6. G. Berden, R. Peeters, G. Meijer, Cavity ring-down spectroscopy: experimental schemes and applications. *Int. Rev. Phys. Chem.* **19**, 565–607 (2000)
7. E. Hawe, P. Chambers, C. Fitzpatrick, E. Lewis, CO₂ monitoring and detection using an integrating sphere as a multipass absorption cell. *Meas. Sci. Technol.* **18**, 3187–3194 (2007)
8. D. Masiyano, J. Hodgkinson, R.P. Tatam, Gas cells for tunable diode laser absorption spectroscopy employing optical diffusers. Part 2: integrating spheres. *Appl. Phys. B* **100**, 303–312 (2010)
9. M. Sjöholm, G. Somesfalean, J. Alnis, S. Andersson-Engels, S. Svanberg, Analysis of gas dispersed in scattering media. *Opt. Lett.* **26**, 16–18 (2001)
10. T. Svensson, E. Adolfsson, M. Lewander, C.T. Xu, S. Svanberg, Disordered, strongly scattering porous materials as miniature multipass gas cells. *Phys. Rev. Lett.* **107**, 143901 (2011)
11. C. Stowasser, A.D. Farinas, J. Ware, D.W. Wistisen, C. Rella, E. Wahl, E. Crosson, T. Blunier, A low-volume cavity ring-down spectrometer for sample-limited applications. *Appl. Phys. B* **116**, 255–270 (2014)
12. T. Gulluk, H.E. Wagner, F. Slemr, A high-frequency modulated tunable diode laser absorption spectrometer for measurements of CO₂, CH₄, N₂O, and CO in air samples of a few cm³. *Rev. Sci. Instrum.* **68**, 230–239 (1997)
13. J. Hodgkinson, R. Smith, W.O. Ho, J.R. Saffell, R.P. Tatam, Non-dispersive infra-red (NDIR) measurement of carbon dioxide at 4.2 μm in a compact and optically efficient sensor. *Sens. Actuators B* **186**, 580–588 (2013)
14. A. O’Keefe, J.J. Scherer, J.B. Paul, CW integrated cavity output spectroscopy. *Chem. Phys. Lett.* **307**, 343–349 (1999)
15. R. Engeln, G. Berden, R. Peeters, G. Meijer, Cavity enhanced absorption and cavity enhanced magnetic rotation spectroscopy. *Rev. Sci. Instrum.* **69**, 3763–3769 (1998)
16. J.B. Paul, L. Lapson, J.G. Anderson, Ultrasensitive absorption spectroscopy with a high-finesse optical cavity and off-axis alignment. *Appl. Opt.* **40**, 4904–4910 (2001)
17. Y.A. Bakhirkin, A.A. Kosterev, C. Roller, R.F. Curl, F.K. Tittel, Mid-infrared quantum cascade laser based off-axis integrated cavity output spectroscopy for biogenic nitric oxide detection. *Appl. Opt.* **43**, 2257–2266 (2004)

18. L. Ciaffoni, J. Couper, G. Hancock, R. Peverall, P.A. Robbins, G.A.D. Ritchie, RF noise induced laser perturbation for improving the performance of non-resonant cavity enhanced absorption spectroscopy. *Opt. Express* **22**, 17030–17038 (2014)
19. K.M. Manfred, J.M.R. Kirkbride, L. Ciaffoni, R. Peverall, G.A.D. Ritchie, Enhancing the sensitivity of mid-IR quantum cascade laser-based cavity-enhanced absorption spectroscopy using RF current perturbation. *Opt. Lett.* **39**, 6811–6814 (2014)
20. Y. Arita, P. Ewart, Multi-mode absorption spectroscopy. *Opt. Commun.* **281**, 2561–2566 (2008)
21. M.L. Hamilton, G.A.D. Ritchie, Y. Arita, P. Ewart, Multi-mode absorption spectroscopy, MUMAS, using wavelength modulation and cavity enhancement techniques. *Appl. Phys. B* **100**, 665–673 (2010)
22. C. Dyroff, Optimum signal-to-noise ratio in off-axis integrated cavity output spectroscopy. *Opt. Lett.* **36**, 1110–1112 (2011)
23. X.T. Lou, G. Somesfalean, Z.G. Zhang, Gas detection by correlation spectroscopy employing a multimode diode laser. *Appl. Opt.* **47**, 2392–2398 (2008)
24. X.T. Lou, G. Somesfalean, S. Svanberg, Z.G. Zhang, S.H. Wu, Detection of elemental mercury by multimode diode laser correlation spectroscopy. *Opt. Express* **20**, 4927–4938 (2012)
25. P. Malara, M.F. Witinski, F. Capasso, J.G. Anderson, P. De Natale, Sensitivity enhancement of off-axis ICOS using wavelength modulation. *Appl. Phys. B* **108**, 353–359 (2012)
26. V.L. Kasyutich, C.E. Canosa-Mas, C. Pfrang, S. Vaughan, R.P. Wayne, Off-axis continuous-wave cavity-enhanced absorption spectroscopy of narrow-band and broadband absorbers using red diode lasers. *Appl. Phys. B* **75**, 755–761 (2002)
27. W. Zhao, X. Gao, W. Chen, W. Zhang, T. Huang, T. Wu, H. Cha, Wavelength modulated off-axis integrated cavity output spectroscopy in the near infrared. *Appl. Phys. B* **86**, 353–359 (2007)
28. G. Somesfalean, M. Sjöholm, L. Persson, H. Gao, T. Svensson, S. Svanberg, Temporal correlation scheme for spectroscopic gas analysis using multimode diode lasers. *Appl. Phys. Lett.* **86**, 184102 (2005)
29. J. Hodgkinson, D. Masiyano, R.P. Tatam, Using integrating spheres with wavelength modulation spectroscopy: effect of pathlength distribution on 2nd harmonic signals. *Appl. Phys. B* **110**, 223–231 (2013)
30. E.J. Moyer, D.S. Sayres, G.S. Engel, J.M.S. Clair, F.N. Keutsch, N.T. Allen, J.H. Kroll, J.G. Anderson, Design considerations in high-sensitivity off-axis integrated cavity output spectroscopy. *Appl. Phys. B* **92**, 467–474 (2008)